

Experimental evidence of modulation instability in a photorefractive $\text{Bi}_{12}\text{TiO}_{20}$ crystal

M. D. Iturbe-Castillo, M. Torres-Cisneros, J. J. Sánchez-Mondragón, S. Chávez-Cerda, S. I. Stepanov, V. A. Vysloukh, and G. E. Torres-Cisneros*

Laboratorio de Fotónica y Física Óptica, Instituto Nacional de Astrofísica, Óptica y Electrónica, Apartado Postal 51, Puebla 72000, México

Received June 7, 1995

We present experimental results on the propagation of an interference pattern of two He–Ne laser beams of unequal amplitudes through a photorefractive $\text{Bi}_{12}\text{TiO}_{20}$ crystal in the presence of drift nonlinearity. The phenomenon that we have observed is the focusing of the fringes as the nonlinearity of the crystal is increased. We show that such a phenomenon can be quantitatively interpreted in the framework of modulation instability theory. © 1995 Optical Society of America

The phenomenon of modulation instability (MI) is characteristic of nonlinear systems. It appears when a cw solution is perturbed with a periodic low-intensity signal, and it causes the generation of sidebands around the cw spectral frequency.¹ The nonlinear Schrödinger equation, which governs the temporal pulse propagation through optical fibers and two-dimensional spatial beam propagation in Kerr-type media, exhibits MI. In the time domain it has been successfully applied to generate periodic arrays of temporal pulses with controllable repetition rates.² In the spatial domain MI together with an effective gain mechanism has given rise to clean arrays of both bright and dark spatial solitons.³ However, Kerr-type media could not be the optimal materials for the practical applications of this and other nonlinear phenomena. This is because of the requirement for laser powers of the order of watts, the length of the nonlinear media, and the availability of materials with positive and negative nonlinear contributions to the refractive index.

On the other hand, currently there is growing interest in two- and three-dimensional beam-propagation problems in photorefractive crystals (PRC's) because they surpass the features of Kerr materials. For example, the first observations of bright^{4,5} and dark^{6,7} spatial solitons in PRC's with different types of nonlinearity have been reported at much lower laser powers (of the order of a milliwatt). The purpose of this Letter is to report experimental evidence and to give a theoretical interpretation of the MI effect in a PRC in the presence of a drift nonlinearity.

The experimental arrangement is shown in Fig. 1. A 10-mW cw He–Ne laser beam was filtered and expanded up to 2-cm diameter. This beam equally illuminated the two mirrors, and the reflected beams were sent to a 9 mm × 5 mm × 2 mm (110)-cut photorefractive $\text{Bi}_{12}\text{TiO}_{20}$ (BTO) crystal. The same crystal was used in our experimental observation of dark spatial solitons.⁷ At the entrance of the crystal the two beams produce an interference pattern with a period depending on the total angle between them. To produce an interference pattern with a fringe visibility of 0.5, we placed a neutral-density filter (0.6 optical

density) in the path of one of the reflected beams. The interference fringes were orthogonal to the direction of the applied voltage to the crystal (its shortest size). An imaging system, consisting of a lens and a CCD camera, was used to analyze the intensity distributions at the input and output faces of the crystal. To control the profile and depth of the refractive-index change in the sample it was necessary to provide uniform illumination at the interelectrode spacing with light coming up from a second 10-mW cw He–Ne laser beam. This beam was sent to the sample by a beam splitter.

The experimental output profiles for three different applied voltages are shown in Fig. 2 for an initial interference pattern with 14 fringes/mm. As one can see, the peak intensity of the fringes increases and their width decreases as the applied voltage is increased. This focusing effect is shown in Fig. 3, where we plot the experimental measurements (open circles) of the fringe peak intensity as the voltage varies. It is worth noting that in addition to the fringe focusing Fig. 2 also shows a space shift of the fringes that is due to the well-known phase transfer phenomenon,⁸ which is essential in the case of gratings produced by beams of different amplitudes.

We now give a theoretical description for the results of Fig. 2. The scalar two-dimensional model of laser beam propagation in a PRC with drift nonlinearity is governed by the standard equation

$$i \frac{\partial A}{\partial Z} = \frac{1}{2} \frac{\partial^2 A}{\partial X^2} + k_0 L_D \delta n A, \quad (1)$$

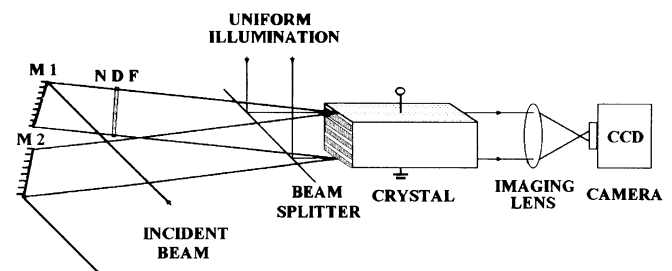


Fig. 1. Diagram of the experimental setup. M1, M2, mirrors; NDF, neutral-density filter.

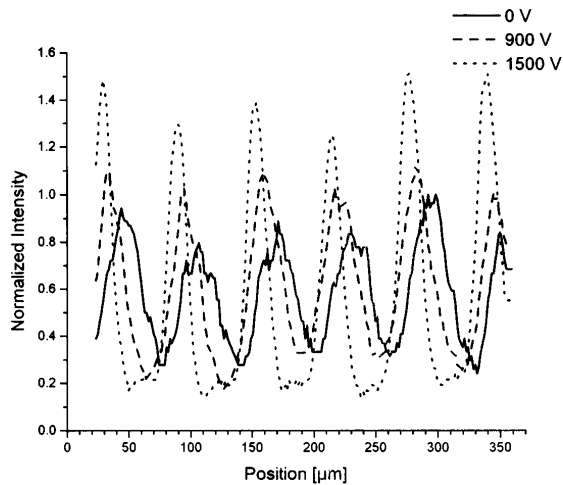


Fig. 2. Experimental output profiles at the indicated voltages when the initial interference pattern has 14 fringes/mm.

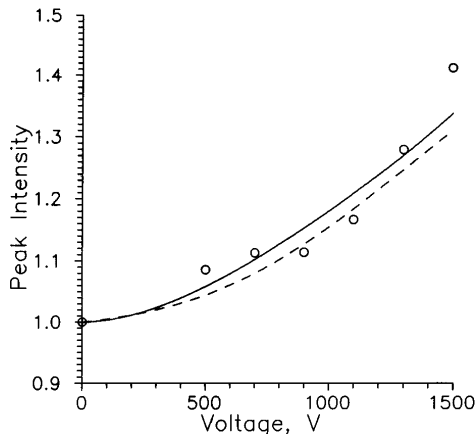


Fig. 3. Experimental (open circles), numerical (solid curve), and theoretical (dashed curve) results for the output fringe peak intensity as a function of the voltage applied to the BTO crystal. The input profile has 14 fringes/mm.

where $A(X, Z)$ is the (slowly varying) beam envelope, k_0 is the wave number, and δn is the nonlinear contribution to the refractive index. $X = x/x_0$ and $Z = z/L_D$, with x_0 being the characteristic transverse scale, $L_D = n_0 k_0 x_0^2$ is the diffraction length, and n_0 is the linear refractive index. The nonlinear change of the PRC refractive index is produced by the electro-optic effect that is due to the presence of the space-charge electric field E_{sc} induced within the crystal⁸: $\delta n(X) = 1/2 r n_0^3 E_{sc}$, where r is the electro-optic coefficient. For a PRC with drift nonlinearity the conductivity σ is supposed to be proportional to the light intensity, which we decompose into the intensity of the uniform illumination, I_0 , and the intensity of the signal itself, $I(X) = |A|^2$. Thus $\sigma = \sigma_0 [I_0 + I(X)]$, where σ_0 is a constant. In steady-state conditions, the unidimensional continuity equation for the current density, $dJ/dX = 0$, establishes that $J(X) = \sigma E_{sc} = J_0$, where J_0 is a constant. Therefore

$$E_{sc} = \frac{J_0}{\sigma_0 [I_0 + I(X)]}. \quad (2)$$

Note that this internal electric field is related to the externally applied voltage through $V_0 = \int_0^L E_{sc} dX$, where L is the transverse width of the crystal. Substituting Eq. (2) into the expression for δn , we obtain

$$\delta n = \pm \delta n_0 \left(1 - \frac{|A|^2/I_0}{1 + |A|^2/I_0} \right), \quad (3)$$

where $\delta n_0 = (1/2) r n_0^3 \tilde{E}$ and $\tilde{E} = V_0/L$. Notice that the sign of δn can be changed by choice of the polarity of the applied voltage. The nonlinear refractive-index change of Eq. (3) is similar to that of the saturable Kerr nonlinearity.⁹ If we define $A(X, Z) = \sqrt{I_m} q(X, Z)$, where I_m is the signal intensity, and neglect the constant term in Eq. (3), which will just introduce a constant in X and a linear-in- Z phase shift, Eq. (1) becomes

$$i \frac{\partial q}{\partial Z} = \frac{1}{2} \frac{\partial^2 q}{\partial X^2} + R \frac{\mu |q|^2}{1 + \mu |q|^2} q, \quad (4)$$

where $\mu = I_m/I_0$ is the saturation parameter and $R = L_D/L_{NL}$, with $L_{NL} = 1/(k_0 \delta n_0)$. For the BTO crystal used in our experiments, $L = 0.2$ cm, $r = 6.175 \times 10^{-10}$ cm/V, and $n_0 = 2.58$; from our experimental setup described above $V_0 \sim 1500$ V, $\mu \sim 1$, and $\lambda = 0.632$ μm ; and we set $x_0 = 50$ μm as the normalization transverse distance. Therefore the appropriate parameters for Eq. (4) are $L_D = 6.45$ cm, $\delta n_0 = 3.975 \times 10^{-5}$, $L_{NL} = 0.251$ cm, and $R = 25.6$.

To simulate our experimental conditions we use

$$q(X, 0) = [1 + a_0 \cos(2\pi X/T)] \exp(-X^6/2b^6), \quad (5)$$

where a_0 and T are, respectively, the modulation amplitude and the normalized period of the fringes and b is the width of the finite background.

In Fig. 4 we show the numerical result of modeling the propagation of an initial profile containing 14 fringes/mm and a visibility of 1/2 ($a_0 = 0.28$) through our 9-mm-long PRC. As one can see, each oscillation of the interference pattern narrows and increases its peak intensity as the propagation takes place. The output profile shows a focusing similar to

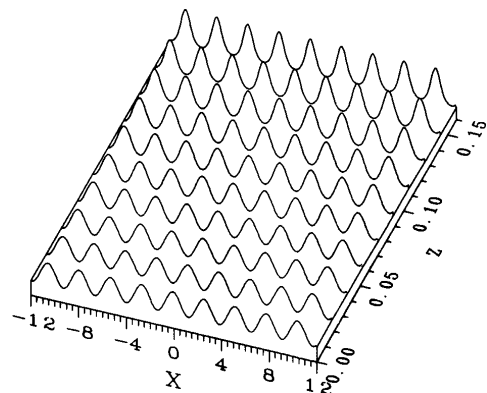


Fig. 4. Numerical result calculated with Eqs. (4) and (5) of modeling the propagation of an interference pattern with 14 fringes/mm through a 9-mm-long BTO crystal. The parameters used were $T = 1.423$, $\mu = 1$, $R = 25.67$, $a_0 = 0.28$, and $b = 20$.

that experimentally obtained with $V = 1500$ in Fig. 2. The solid curve in Fig. 2 represents the output fringe peak intensity numerically obtained as the voltage is varied. Note that this curve is in good agreement with the experimental results (open circles).

The focusing process plotted in Fig. 4 does not continue indefinitely. Instead, our numerical results show that it stops at some propagation distance, and then the fringe width increases and its peak intensity decreases, recovering its initial values, provided that $b \gg T$. Thus the propagation of an initial oscillatory profile is characterized by a recurrent behavior, similar to that found for the nonlinear Schrödinger equation when an infinite oscillatory profile is used.¹⁰ This periodic focusing and defocusing of the initial oscillatory profile can be explained in terms of the phasing and dephasing within the nonlinear medium of the initial two spectral components with the additional ones generated by the MI effect.¹⁰

The initial stage of this process can be qualitatively described by perturbation of Eq. (4). We first note that Eq. (4) accepts the plane-wave solution $q(X, Z) = q_0 \exp(i\phi_{\text{NL}}Z)$, where $\phi_{\text{NL}} = R\mu q_0^2/(1 + \mu q_0^2)$. Now if we perturb this solution in the form $q = (q_0 + \delta q) \exp(i\phi_{\text{NL}}Z)$, the perturbation satisfies the linearized dynamic equation

$$i \frac{\partial \delta q}{\partial Z} = \frac{1}{2} \frac{\partial^2 \delta q}{\partial X^2} + 2Rf(\mu)\text{Re}(\delta q), \quad (6)$$

where $f(u) = \mu q_0^2/(1 + \mu q_0^2)^2$ is a weight function. If we assume a periodic perturbation, $\delta q = C \cos(KZ - \Omega X) + iD \sin(KZ - \Omega X)$, then K becomes imaginary and the perturbation will grow for perturbation frequencies satisfying $\Omega < \Omega_c = 2\sqrt{Rf(\mu)}$. For $\Omega < \Omega_c$, the associated gain coefficient is given by $\alpha = 2 \text{Im}(K) = \Omega \sqrt{\Omega_c^2 - \Omega^2}$. These results indicate that both the gain bandwidth and the gain magnitude depend on μ . They reach their maximum values, $\Omega_{c,\text{max}} = \sqrt{R}$ and $\alpha_{\text{max}} = \sqrt{R}/2$, respectively, at $\mu q_0^2 = 1$. Note that for our experimental and numerical results we are using $\mu q_0^2 \sim 1$ and, therefore, $\Omega_c \sim 5$, which corresponds to an interference pattern with 16 fringes/mm.

When $\Omega < \Omega_c$, and for the initial condition given by Eq. (5) with $b \rightarrow \infty$, the solution for the perturbation δq can be written as

$$\begin{aligned} \delta q = & a_0 \cosh(\alpha Z/2) \cos(\Omega X) - i(a_0 \alpha/2\Omega^2) \\ & \times \sinh(\alpha Z/2) \cos(\Omega X). \end{aligned} \quad (7)$$

The dashed curve in Fig. 3 represents the behavior of $|1 + \delta q|^2$, with $a_0 = 0.28$, as the voltage applied to the crystal is varied. As one can see, there is reasonably good agreement of Eq. (7) with both experimental and numerical results.

In summary, we have presented experimental results that reveal the onset of the modulation instability effect in photorefractive crystals in the presence of drift nonlinearity. This result opens the possibility of carrying out experimental studies similar to those in Kerr media^{2,3} at much lower laser powers and with more practical perspectives.

This research was partially supported by the Consejo Nacional de Ciencia y Tecnología under grant F388-E. We express our sincere gratitude to M. Klein and B. Wechsler of Hughes Research Laboratories for permission to use their BTO samples in these experiments.

*Permanent address, Facultad de Ingeniería Mecánica, Eléctrica y Electrónica, Universidad de Guanajuato, Apartado Postal 215-A, Salamanca, GTO 36730, Mexico; and Academic Adviser, Grupo Educativo IMA, s.c., Apartado Postal 172, Cortazar, GTO 38301, México.

References

1. V. I. Vespilov and V. I. Talanov, *Sov. Phys. JETP Lett.* **3**, 307 (1966).
2. A. Hasegawa, *Opt. Lett.* **9**, 288 (1984).
3. E. M. Dianov, P. V. Mamyshev, A. M. Prokhorov, and S. V. Chernikov, *Opt. Lett.* **14**, 1008 (1989); P. V. Mamyshev, Ch. Bosshard, J. Wilson, and G. I. Stegeman, *J. Opt. Soc. Am. B* **11**, 1254 (1994).
4. G. C. Duree, J. L. Shultz, G. J. Salamo, M. Segev, A. Yariv, B. Crosignani, P. DiPorto, E. J. Sharp, and R. R. Neurgaonkar, *Phys. Rev. Lett.* **71**, 533 (1993).
5. M. D. Iturbe-Castillo, P. A. Márquez-Anguilar, J. J. Sánchez-Mondragón, S. Stepanov, and V. Vysloukh, *Appl. Phys. Lett.* **64**, 484 (1994).
6. M. Segev, G. Salamo, G. Duree, M. Morin, B. Crosignani, P. Di Porto, and A. Yariv, *Opt. Photon. News* **5**(12), 9 (1994).
7. M. D. Iturbe-Castillo, J. J. Sánchez-Mondragón, S. I. Stepanov, M. B. Klein, and B. A. Wechsler, "(1 + 1)-dimensional dark spatial soliton in photorefractive Bi₁₂TiO₂₀ crystal," *Opt. Commun.* (to be published).
8. M. P. Petrov, S. I. Stepanov, and A. V. Khomenko, *Photorefractive Crystals in Coherent Optical Systems* (Springer-Verlag, Heidelberg, 1991), Chap. 6.
9. Ya. B. Zel'dovich and Yu. P. Raizer, *JETP Lett.* **3**, 86 (1966); Y. Chen, *Opt. Lett.* **16**, 4 (1991).
10. S. Trillo and S. Wabnitz, *Opt. Lett.* **16**, 986 (1991).